Application of the chiral forces to elctroweak processes

Vitalii Urbanevych

Ph.D. thesis written under the supervision of dr. hab Roman Skibiński
at the Jagiellonian University, Faculty of Physics, Astronomy
and Applied Computer Science, Kraków,
Sunday 3rd October, 2021

CONTENTS

CHAPTER 1

PLAN

- Why we study few nucleon systems
  - Strong interactions (2N and 3N force investigation; QCD, relativistic effects)
  - Electro-magnetic processes (electrons-, photons-induced reactions) (Arenhovel did ...)
  - Weak interactions (neutrons)
- Nuclear forces used in the thesis
  - AV18
  - Chiral (scs, sms; difference between chiral models; regularization problem)
- Currents used in the thesis (regularization of currents to be done)
- Formalism & numerical methods
  - Lippman-Schwinger eq
  - Schrodinger eq for deuteron; wave functions (sms) for deuteron - figures, binding energy
  - Three body: Fadeev eq. for bound (He3, H3) and scattering states
  - Siegert theorem ?
  - Partial wave decomposition, states ($pq\alpha$), Jakobi momenta; operators in PW decomp. (current); Mathematica for PW
  - Theoretical uncertainties: truncation error, cut-off dependency, chiral order dependency
- Results (**find everything what I have calculated: all processes and energies**)
  - H2 photodisintegration
  - He3 and H3 photodisintegration
  - Pion capture

- Summary
- References

Why we study few nucleon systems

The study of light nuclei for the decades has been serving as an easiest way to study NN systems and forces inside the atom. And convenient way to proceed may be an interaction of atom with other particles: elastic or inelastic scattering. It is possible to construct such an experiments and check if theory works. People take into account that interactions may be caused by different forces and therefore should be described in different ways. It can be either strong, weak or electromagnetic interaction. It depends on the type of particle being scattered and the target which reaction it is.

In order to proper describe the nuclear reactions many factors should be taken into account. First of all, different nuclear forces may act on the participants.

The strong nuclear force appear inside the nuclei and among others bound neutrons and protons together. The description of strong interactions is extremely difficult as it deals not only with nucleon, but with their constituents: quarks and gluons. Quantum Chromodynamics(QCD) is a modern theory describing strong interactions, but it has also its limitations at the moment as it is not reliable at low energies ($Q^2 \lesssim 1GeV^2$). So other approaches are coming into the scene such as chiral effective theory, lattice calculation and others [1].

Electromagnetic force appears between charged particles like protons and electrons. Also, the force is transferred between charged particles with a photon, so in photon- and electron- scatterings on the nuclei an electromagnetic force is playing an important role. Arenhovel [2] studied electromagnetic process - Deuteron photodisintegration, applying different approaches and comparing the results with experimental data.

The weak force...

...

Starting the study of 3- (and more) nucleon systems it was found that 2N force is not enough to describe the system and 3N force was introduced. The first applications of such a force showed that it brings sufficient contribution and cannot be ignored [3]. Whereas the first applications included only early "realistic" potential, the latter investigations only proved this statements [4, 5]. It was also used to construct four-nucleon (4N) bound state [6].

...

Nuclear forces used in the thesis

In order to construct a potential people often use phenomenological or semi-phenomenological approaches. It allows to combine theoretical knowledge about processes and experimental data.

One of such potentials, which was used in current thesis is Argonne V18 (AV18) [7] In order to construct NN force, authors combine analytical electromagnetic and one-pion-exchange parts with phenomenological one, fitting parameters to the Nijmegen partial-wave analysis of *pp* and *np* data [8]. Authors showed, that AV18 potential delivers good results in the description of nucleon scattering data as well as deuteron properties.

In the early 1990-ies Weinberg [9, 10] introduced an idea of using a most general Lagrangian satisfying assumed symmetry principles and in particular spontaneously bro-

ken chiral symmetry to describe nuclear interactions at low energies. This idea together with effective field theory (EFT) of Quantum chromodynamics (QCD) led to the development of Chiral effective field theory (χEFT) which nowadays has become one of the most advanced approach to describing nuclear reactions at low energies.

For the EFT it is very important to define a quantity, which powers will determine a perturbation order. In the χEFT there are two natural scales: so-called soft scale - the mass of Pion $Q \sim M_\pi$ and hard scale - $\Lambda_\chi \sim 1\ GeV$ (chiral symmetry breaking scale). The ratio between these two scales $(Q/\Lambda_\chi)^\nu$ is being used as an expansion parameter in χEFT with power ν.

Considering so-called irreducible (the diagrams that cannot be split by cutting nucleon lines), Weinberg [9, 10] came to the identity for the powers of such diagrams[11]:

$$\nu_W = 4 - A - 2C + 2L + \sum_i \Delta_i, \tag{1.1}$$

where

$$\Delta_i \equiv d_i + \frac{n_i}{2} - 2 \tag{1.2}$$

In 1.1, C is a number of pieces which are connected, L - the number of loops in the graph. In 1.2, n_i is a number of nucleon field operators, d_i - the number of insertions (or derivatives) of M_π.

In χEFT the first order is called "leading order" (LO) and it is followed by next-to-leading order (NLO), next-to-next-to-leading order (N2LO) and so on. At the moment, the highest order for which there is a derived term in potential is N4LO. Also some contributions from N5LO are included in the N4LO+ chiral order.

As pointed above, for many-nucleon systems it is important to include not only nucleon-nucleon interaction to the potential, but also a 3- and many- nucleon contributions. In the χEFT 3N force contributes starting from N2LO and 4N force is presented starting from N3LO, so there is a systematic way to include all the forces from simplest diagrams at LO and gradually adding more and more terms. It is also beneficial in the way that one can obtain results using chiral potential at different orders and track which one gives larger or smaller contribution (changes in the final results).

The χEFT may be applied both in coordinate and momentum spaces. Nevertheless in both cases it requires regularization which is cutting low coordinate values in order to avoid infinities (or high momentum values - in momentum space). The value at which the cut is applied (cut-off value) is not fixed and usually calculations are being performed for different cut-off values. The comparison of such results may reveal stronger or weaker dependance and in perfect case one will come up with such a potential, were the cut will not affect results much.

The potential may be transformed from coordinate to momentum space (or vice versa), but it is important at which frame the regularization was performed and what was a regularization function. That's why there are different versions of chiral potential. One is semi-local coordinate space regularized potential (SCS) [12] and another one is similar, but with regularization applied in momentum space (SMS potential) [13].

Currents

CHAPTER 2

FORMALISM & NUMERICAL METHODS

In order to calculate any observable for the Deuteron photodisintegration, one has to find a nuclear matrix elements:

$$N^{\mu} = \langle \Psi_f \vec{P_f} \mid \frac{1}{e} J^{\mu}(0) \mid \Psi_i \vec{P_i} \rangle = \langle p'(l's')j'm'_j t'm'_t \vec{P_f} \mid J^{\mu} \mid \phi_d m_d \vec{P_i} \rangle, \tag{2.1}$$

where J^{μ} is a four-vector current operator which acts between initial and final two-nucleon states.

2.1 Deuteron bound state

Let's find a deuteron bound state wave function ϕ_d. The time-independent Schrodinger equation for two particles in such case will be:

$$(H_0 + V) \mid \psi_{12} \rangle = E_d \mid \psi_{12} \rangle \tag{2.2}$$

H_0 is a kinetic energy of the nucleons and V is a potential. The kinetic energy H_0 can be represented in terms of relative and total momenta of the particles:

$$H_0 = \frac{\vec{p_1}^2}{2m_1} + \frac{\vec{p_2}^2}{2m_2} = \frac{\vec{p}^2}{2\mu} + \frac{\vec{\mathcal{P}}^2}{2M}, \tag{2.3}$$

where relative and total momenta are defined as follows:

$$\vec{p} = \frac{(m_1\vec{p_1} - m_2\vec{p_2})}{m_1 + m_2} \tag{2.4}$$

$$\vec{\mathcal{P}} = \vec{p_1} + \vec{p_2} \tag{2.5}$$

and $M = m_1 + m_2$ is a total mass, $\mu = \frac{m_1 m_2}{M}$ is a relative mass of two nucleons.

We are working in the momentum space, so acting by the momentum operator on the Eq.2.2 one can obtain two separated equations:

$$\frac{\vec{p}^2}{2\mu}\langle\vec{p}\mid\Psi_{int}\rangle+\int d\vec{p}'\langle\vec{p}\mid V\mid\vec{p}'\rangle\langle\vec{p}'\mid\Psi_{int}\rangle=(E_d-E_{c.m.})\langle\vec{p}\mid\Psi_{int}\rangle \tag{2.6}$$

$$\frac{\vec{\mathcal{P}}^2}{2M}\langle\mathcal{P}\mid\Psi_{c.m.}\rangle=E_{c.m.}\langle\mathcal{P}\mid\Psi_{c.m.}\rangle \tag{2.7}$$

Eq.2.6 is basically a Schrodinger equation for one particle with mass μ and Eq.2.7 can be regarded as a Schrodinger equation for particle with mass M in a free motion. Assuming that deuteron is at rest ($E_{c.m.}=0$) we can stick to the Eq.2.6 only. So that:

$$\frac{\vec{p}^2}{2\mu}\langle\vec{p}\mid\Psi_{int}\rangle+\int d\vec{p}'\langle\vec{p}\mid V\mid\vec{p}'\rangle\langle\vec{p}'\mid\Psi_{int}\rangle=E_d\langle\vec{p}\mid\Psi_{int}\rangle \tag{2.8}$$

Next we move to the partial-wave representation of the momentum state in the following form:

$$\mid\vec{p}\rangle=\mid p\alpha\rangle\equiv\mid p(ls)jm_j\rangle\mid tm_t\rangle, \tag{2.9}$$

where we introduce quantum numbers l, s ,j ,t as orbital angular momentum, total spin, total angular momentum and total isospin respectively. m_j and m_t are isospin and spin projections.

Yet one can introduce simpler states than it is in 2.9.

$$\mid p(ls)jm_j\rangle=\sum_{m_l}c(lsj;m_l,m_j-m_l,m_j)\mid plm_l\rangle\mid s\ m_j-m_l\rangle \tag{2.10}$$

Also we can decompose spin and isospin states as follows:

$$\mid sm_s\rangle=\sum_{m_1}c(\frac{1}{2}\frac{1}{2}s;m_1,m_s-m_1,m_s)\mid\frac{1}{2}m_1\rangle\mid\frac{1}{2}m_s-m_1\rangle \tag{2.11}$$

$$\mid tm_t\rangle=\sum_{\nu_1}c(\frac{1}{2}\frac{1}{2}t;\nu_1,m_t-\nu_1,m_t)\mid\frac{1}{2}\nu_1\rangle\mid\frac{1}{2}m_t-\nu_1\rangle \tag{2.12}$$

In Eqs.2.10 -2.12, $c(...)$ are Clebsh-Gordon coefficients. Nucleons are spin $\frac{1}{2}$ particles, and also we treat proton and neutron as the same particle in different isospin states, so that isospin is $\nu_1=\frac{1}{2}$ for proton and $\nu_1=-\frac{1}{2}$ for neutron.

The states $\mid plm_l\rangle$ from Eq.2.10 are orthogonal, so that

$$\langle p'l'm_l'\mid plm_l\rangle=\frac{\delta(p-p')}{p^2}\delta_{ll'}\delta_{m_lm_l'} \tag{2.13}$$

and also satisfy the completeness relation:

$$\sum_{l=0}^{\infty}\sum_{m_l=-l}^{l}\int dpp^2\mid plm_l\rangle\langle plm_l\mid=\mathbb{1} \tag{2.14}$$

These states also fulfill a relation

$$\langle\vec{p}'\mid plm_l\rangle=\frac{\delta(|\vec{p}'|-p)}{p^2}Y_{lm_l}(\hat{p}'), \tag{2.15}$$

where $Y_{lm_l}(\hat{p}')$ is a spherical harmonic and 'hat' means a unit vector.

If we exchange nucleons 1 and 2 there should be a sign change and this requirement can in mathematical form can be expressed as:

$$(-1)^{l+s+t} = -1 \tag{2.16}$$

Taking into account Eq.2.16, one can find only one possible case for the deuteron bound state: 2 coupled channels for l=0,2; s=1; j=1and $t = m_t = 0$. These 2 channels are usually denoted as ${}^3S_1$ and ${}^3D_1$ and corresponding wave functions are $\phi_0(p)$ and $\phi_2(p)$.

So with a new basis Eq.2.8 takes a form:

$$\frac{\vec{p}^2}{2\mu}\phi_l(p) + \sum_{l'=0,2}\int dp' p'^2 \langle p l m_l \mid V \mid p' l' m_l' \rangle \phi_{l'}(p) = E_d \phi_l(p), \tag{2.17}$$

for $l = 0, 2$. Assuming that one has a matrix elements for the potential $\langle p l m_l \mid V \mid p' l' m_l' \rangle$, there is still one complication in the Eq.2.17 - integration. In order to get rid of the integral I use a Gaussian quadrature method of numerical integration [14]. It allows to replace an integral by the weighted sum: $\int_a^b f(x)dx = \sum_{i=1}^n \omega_i f(x_i)$ In current work I used 72 points in the interval from 0 to $50fm$. Using this method, Eq.2.8 becomes

$$\frac{\vec{p}^2}{2\mu}\phi_l(p) + \sum_{l'=0,2}\sum_{j=0}^{N} \omega_j p_j'^2 \langle p_j l m_l \mid V \mid p_j' l' m_l' \rangle \phi_{l'}(p) = E_d \phi_l(p), \tag{2.18}$$

It is possible to solve this equation as an eigenvalue problem $M\Psi = E_n\Psi$ and find simultaneously wave function values and binding energy E_n.

2.2 The Lippman-Schwinger equation

Let us start from the time-independent formulation of the scattering process. In such a case Hamiltonian will be:

$$H = H_0 + V, \tag{2.19}$$

where H_0 is a kinetic energy operator $H_0 = \frac{\vec{p}^2}{2m}$. For a free particle motion, V will be absent and we will denote an energy eigenstate as $\mid \vec{p} \rangle$ - a free particle state. In the case of the scattering process, the eigenstate will differ from $\mid \phi \rangle$, but in case of elastic scattering (which we re interested in) the energy eigenvalue E should be the same.

So below I write a system of Schrodinger equations for such scattering process:

$$\begin{cases} H_0 \mid \vec{p} \rangle & = E \mid \vec{p} \rangle \\ (H_0 + V) \mid \psi \rangle & = E \mid \psi \rangle \end{cases} \tag{2.20}$$

I would like to find such a solution to Eq. 2.20, so that $\mid \psi \rangle \rightarrow \mid \vec{p} \rangle$ with $V \rightarrow 0$ and both $\mid \psi \rangle$ and $\mid \vec{p} \rangle$ have the same energy eigenvalues E. As we have scattering process, the energy spectra for both operators H_0 and$H_0 + V$ are continuous.

From Eq. 2.20 follows that

$$\mid \psi \rangle = \frac{1}{E - H_0} V \mid \psi \rangle + \mid \vec{p} \rangle, \tag{2.21}$$

where $\mid \psi \rangle$ was added artificially in order to satisfy a criterion mentioned above and

following the logic from [15]. In addition, applying the operator $(E - H_0)$ to the 2.21 results in the second equation from the system 2.20.

In order to deal with a singular operator $\frac{1}{E-H_0}$ in eq.2.21, the well-known technique is to make such an operator slightly complex by adding small imaginary number to the denominator making it $\frac{1}{E\pm i\epsilon-H_0}$.

$$\mid \psi\rangle = \frac{1}{E \pm i\epsilon - H_0} V \mid \psi\rangle + \mid \vec{p}\rangle, \tag{2.22}$$

Eq. 2.22 is known as a Lippman-Schwinger equation.

Let me move to the coordinate representation of the Eq. 2.22:

$$\langle \vec{x} \mid \psi\rangle = \langle \vec{x} \mid \frac{1}{E \pm i\epsilon - H_0} V \mid \psi\rangle + \langle \vec{x} \mid \vec{p}\rangle \tag{2.23}$$

If we choose $|\vec{x}\rangle$ to be normalized as $\langle \vec{x}'|\vec{x}\rangle = \delta^3(\vec{x}' - \vec{x})$, the Fourier transform will give us [16]:

$$\langle \vec{x}|\vec{p}\rangle = \frac{1}{(2\pi)^{3/2}} e^{i\vec{p}\cdot\vec{x}}. \tag{2.24}$$

I can rewrite Eq. 2.23 as:

$$\langle \vec{x} \mid \psi\rangle = \int d^3\vec{x}' G(\vec{x}, \vec{x}') \langle \vec{x}'|V|\psi\rangle + \langle \vec{x}|\vec{p}\rangle \,, \tag{2.25}$$

with $G(\vec{x}, \vec{x}')$ denoting a Green function:

$$G(\vec{x}, \vec{x}') = \left\langle \vec{x} \middle| \frac{1}{E \pm i\epsilon - H_0} \middle| \vec{x}' \right\rangle, \tag{2.26}$$

One shall mention, that dealing with the plane-wave state in coordinate space is not normalizable, as it is not a Hilbert vector [15], anyway we imply the "normalization" rule $\int d^3\vec{x} \langle \vec{p}|\vec{x}\rangle \langle \vec{x}|\vec{p}'\rangle = \delta^3(\vec{p} - \vec{p}')$.

The Green function Eq.2.26 can be written in the momentum basis as:

$$G(\vec{x}, \vec{x}') = \frac{1}{(2\pi)^3} \int d^3\vec{p}' \frac{e^{i\vec{p}''\cdot(\vec{x}'-\vec{x})}}{E \pm i\epsilon - \frac{\vec{p}''^2}{2m}}, \tag{2.27}$$

Integration in the 2.27 can be done applying residual technique and here comes the main profit of the $\pm i\epsilon$ in the denominator. The final expression of the Green function will be:

$$G(\vec{x}, \vec{x}') = -\frac{m}{4\pi} \frac{e^{\pm i\sqrt{mE}|\vec{x}'-\vec{x}'|}}{|\vec{x}' - \vec{x}'|} \tag{2.28}$$

The $(\pm)$ in the exponent specifies outgoing and incoming plane-waves. For a scattering particle we are interested in the outgoing wave, so let's stick to the positive sign in the exponent and assume that corresponding wave function is $\psi^{(+)}$.

Let;s assume that potential V is local: $\langle \vec{x}'|V|\vec{x}'\rangle = \delta(\vec{x}' - \vec{x}')V(\vec{x}')$. Then using this assumption and applying Eq.2.28 and Eq.2.24 to Eq.2.25 one gets:

$$\langle \vec{x} \mid \psi^{(+)}\rangle \equiv \psi^{(+)}(\vec{x}) - \frac{m}{4\pi} \int d^3\vec{x}' \frac{e^{\pm i\sqrt{mE}|\vec{x}'-\vec{x}'|}}{|\vec{x}' - \vec{x}'|} V(\vec{x}')\psi^{(+)}(\vec{x}') + \langle \vec{x}|\vec{p}\rangle \,, \tag{2.29}$$

which may be written in the asymptotic form (when $|\vec{x}| \to \infty$) as:

$$\psi^{(+)}(\vec{x}) \to \frac{1}{(2\pi)^{1/3}} \left(e^{i\vec{p}\cdot\vec{x}} + \frac{e^{i\vec{p}\cdot\vec{x}}}{\vec{x}} f(\hat{x}) \right) \tag{2.30}$$

From the Eq. 2.30 one can conclude that at large distances we obtain a wave function which consists of the original plane wave plus an outgoing spherical wave with a scattering amplitude $f(\hat{x})$:

$$f(\hat{x}) \equiv -m\sqrt{\frac{\pi}{2}} \int d^3x' e^{-ip\hat{x}\cdot\vec{x}'} V(\vec{x}')\psi^{(+)}(\vec{x}') \tag{2.31}$$

With substitution a scattered momentum $\vec{p}' \equiv p\hat{x}$ into Eq. 2.31, we can simplify it and get a matrix element of the transition operator t:

$$\langle \vec{p}'|t|\vec{p}\rangle \equiv \frac{1}{(2\pi)^{1/3}} \int d^3x' e^{-i\vec{p}'\cdot\vec{x}'} V(\vec{x}')\psi^{(+)}(\vec{x}') = \left\langle \vec{p}' \middle| V \middle| \psi^{(+)} \right\rangle \tag{2.32}$$

Combining Equations 2.32 and 2.22 one can obtain:

$$t\,|\vec{p}\rangle = V\,|\vec{p}\rangle + VG_0V\left|\psi^{(+)}\right\rangle = V\,|\vec{p}\rangle + VG_0t\,|\vec{p}\rangle\,, \tag{2.33}$$

or in the operator form:

$$t = V + VG_0t \tag{2.34}$$

Practical application Eq.2.34 has mostly in the iterative form. It is a Born series with respect to power of potential V and can be interpreted as taking into account more and more vertices of the rescattering process:

$$t = V + VG_0(V + VG_0t) = V + VG_0V + VG_0VG_0V + ... \tag{2.35}$$

Substitution of Eq.2.33 into Eq.2.1 ...

CHAPTER 3

PION ABSORPTION AT THE LOWEST ATOMIC ORBITAL IN ^{2}H, ^{3}H AND ^{3}HE

CHAPTER 4

RESULTS

4.1 Deuteron photodisintegraion

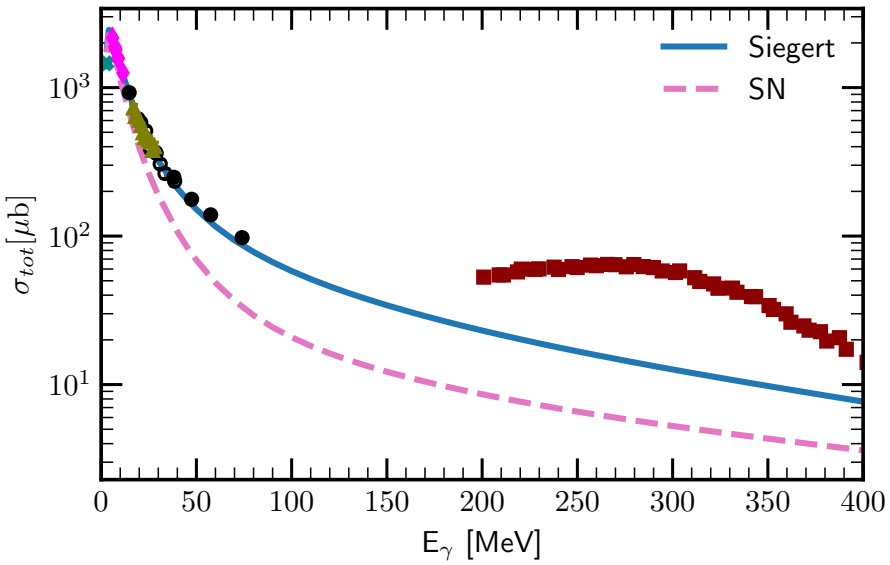

Figure 4.1: Total cross section as a function of the photon's energy E_γ. Solid blue line presents results obtained with SN+Siegert and dashed pink line - with only SN current. The experimental data are from [17] (black filled circles), [18] (empty circles), [19] (red squares), [20] (olive triangles), [21] (cyan crosses X) and [22] (magenta dimonds).

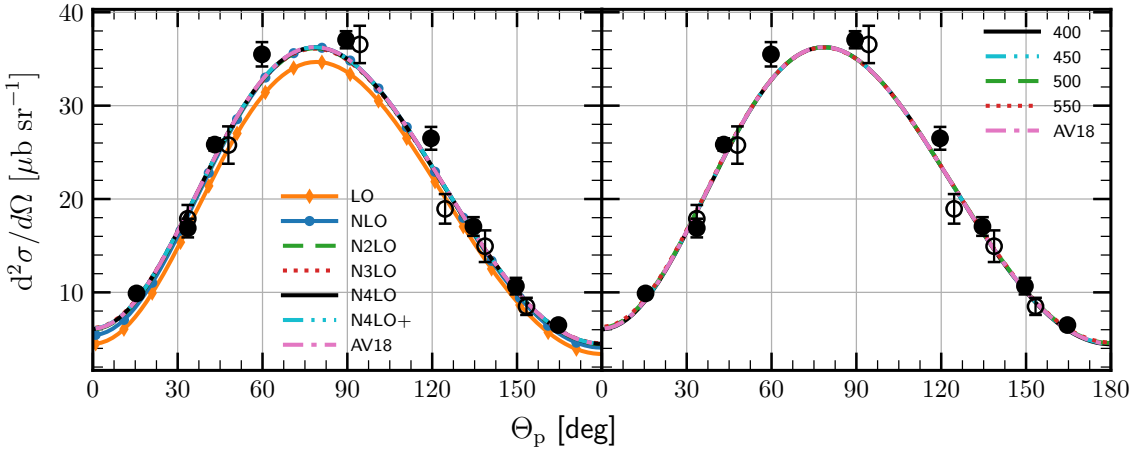

Figure 4.2: Differential cross section as a function of the outgoing proton angle in the center of mass frame for the photon's energy 30 MeV. Left figure presents results obtained using potential with different chiral orders (from LO to N^{4}LO+) with cutoff parameter Λ = 450 MeV whereas right figure presents a cutoff dependency and chiral potential N^{4}LO+ was used in all cases. For the sake of comparison, predictions obtained with AV18 potential are on both figures as well. Data points (filled and empty circles) are from [23].

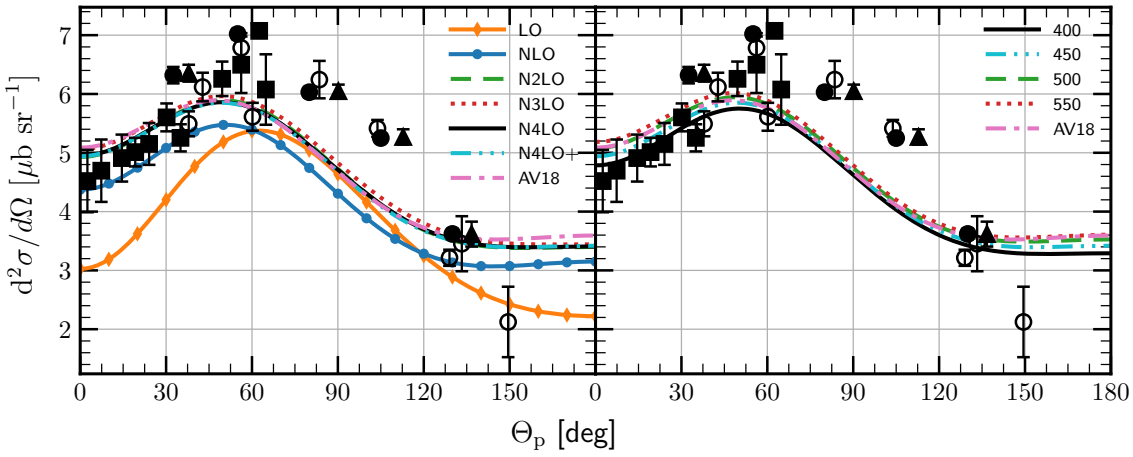

Figure 4.3: The same as on the Fig. 4.2 but for the photon's energy E$_\gamma$=100 MeV. All experimental data points (filled and empty circles, squares and triangles) are from [23].

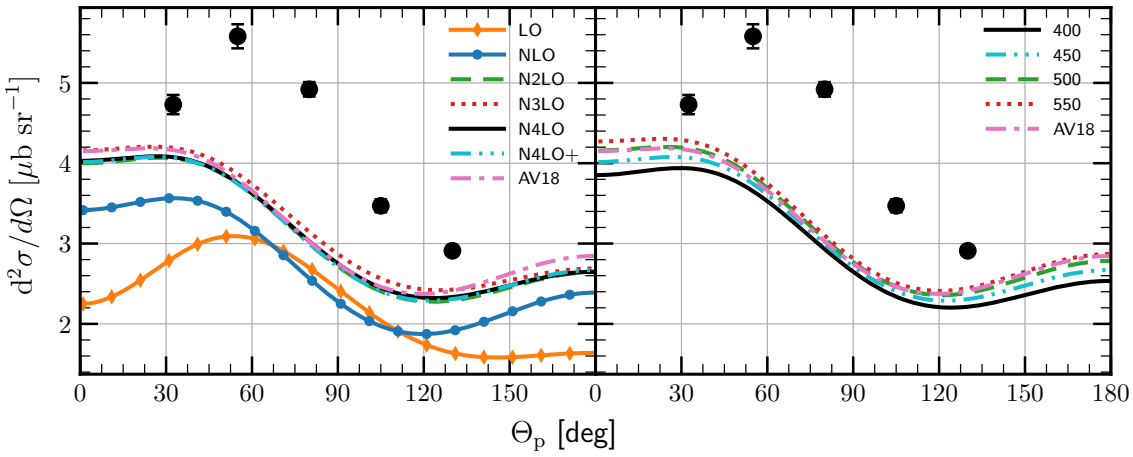

Figure 4.4: The same as on the Fig. 4.2 but for the photon's energy E_γ=140 MeV. The data are from [24].

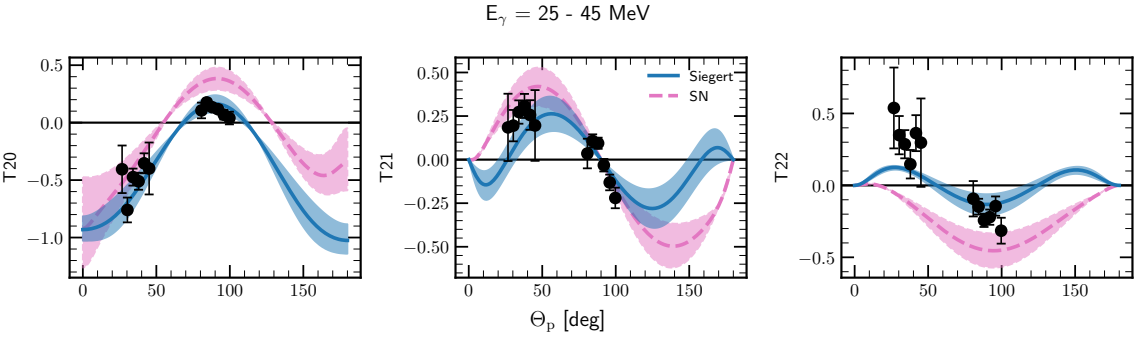

Figure 4.5: Tensor analyzing powers T_{20}, T_{21} and T_{22} as a functions of the outgoing proton angle θ_p (in the center of mass frame). Solid blue line is a mean value of my predictions obtained with a SMS potential at N^{4}LO+ chiral order and with Λ = 450 MeV at energy values from 25 to 45 MeV and where SN current was used together with Siegert approach. Pink dashed line is similar prediction but with SN only. The corresponding bands show the deviation of predictions in the regarded energy region. Filled circles are experimental data from [26] for the analogous energy span.

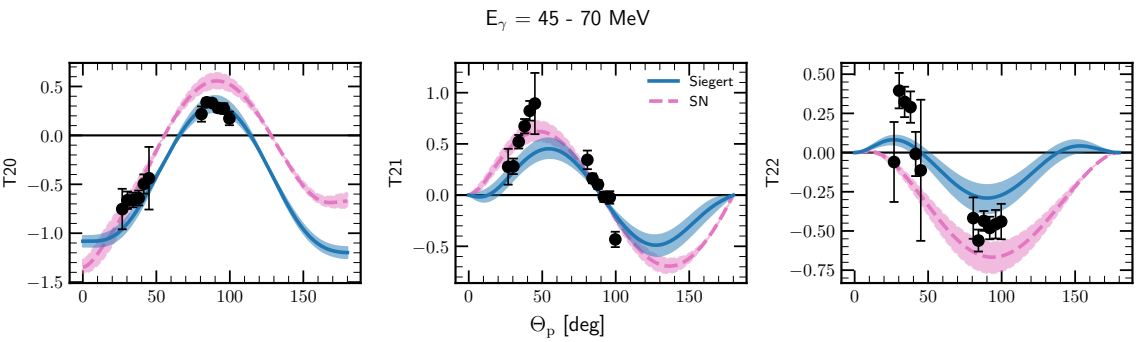

Figure 4.6: The same as on the Fig. 4.5 but for energy bin 45 - 70 MeV

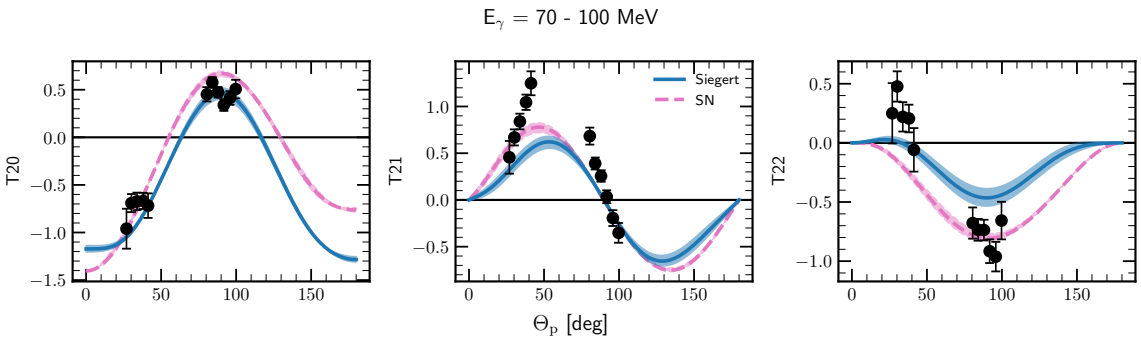

Figure 4.7: The same as on the Fig. 4.5 but for energy bin 70 - 100 MeV

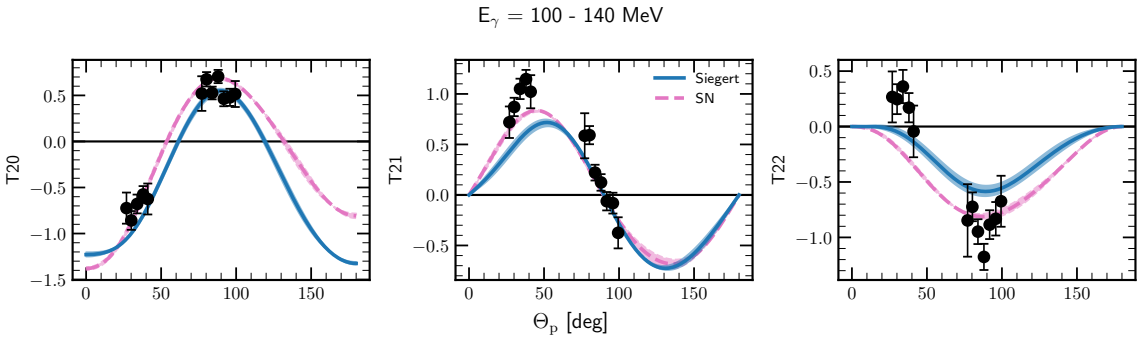

Figure 4.8: The same as on the Fig. 4.5 but for energy bin 100 - 140 MeV

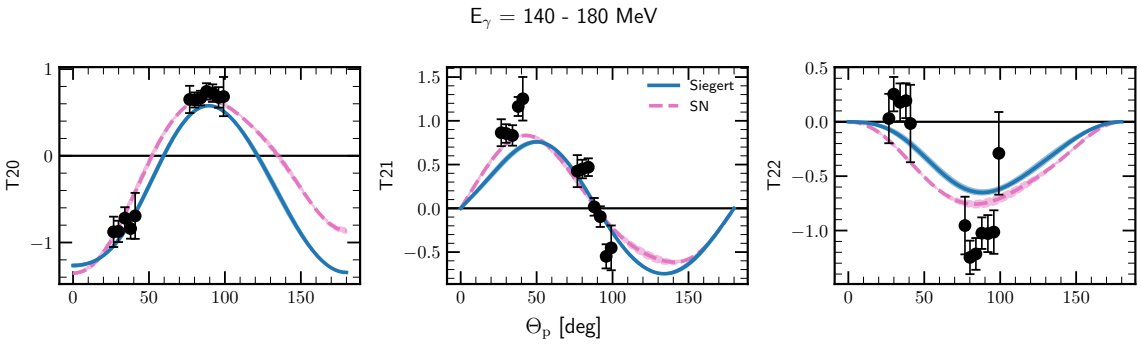

Figure 4.9: The same as on the Fig. 4.5 but for energy bin 140 - 180 MeV

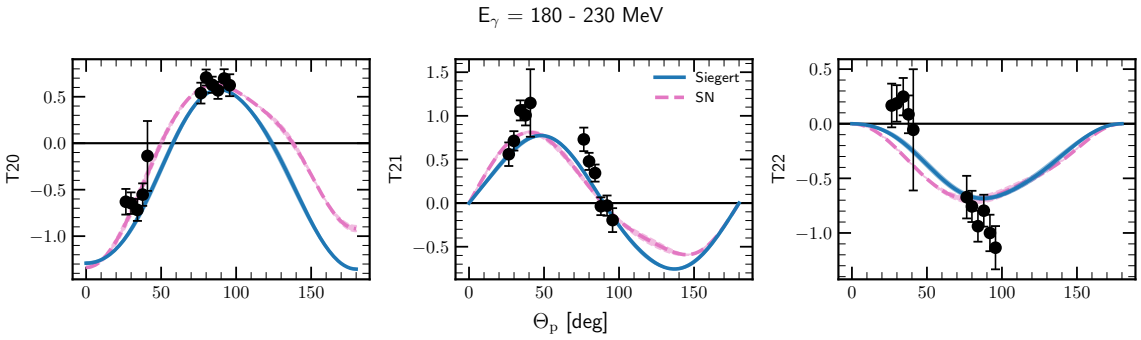

Figure 4.10: The same as on the Fig. 4.5 but for energy bin 180 - 230 MeV

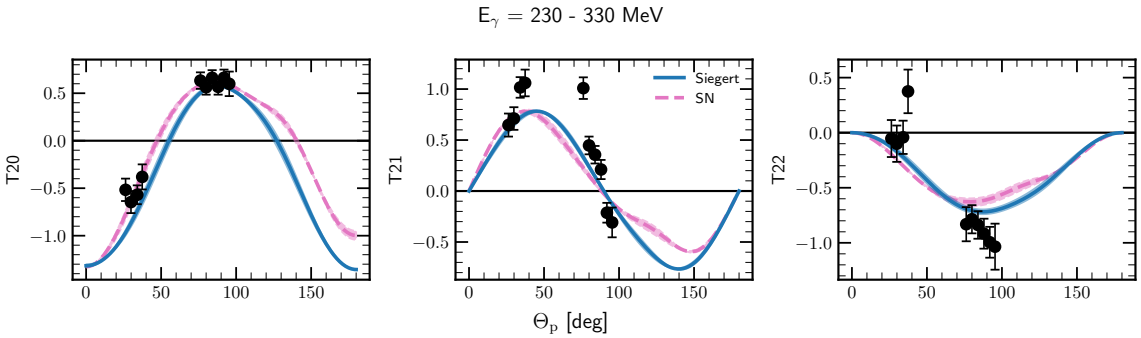

Figure 4.11: The same as on the Fig. 4.5 but for energy bin 230 - 330 MeV

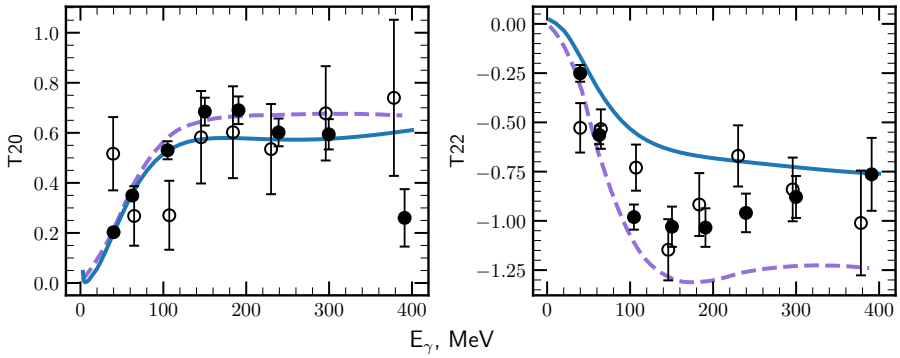

Figure 4.12: Tensor analyzing powers T_{20} and T_{22} as a functions of the photon energy E_γ with fixed outgoing proton angle $\theta_p = 88°$ (in the center of mass frame). My predictions (blue solid line) are obtained with SMS potential at chiral order N^{4}LO+ and with cutoff parameter $\Lambda = 450$ MeV. Dashed purple line presents calculations from [25]. Experimental data is taken from [26] (filled circles) and [27] (empty circles).

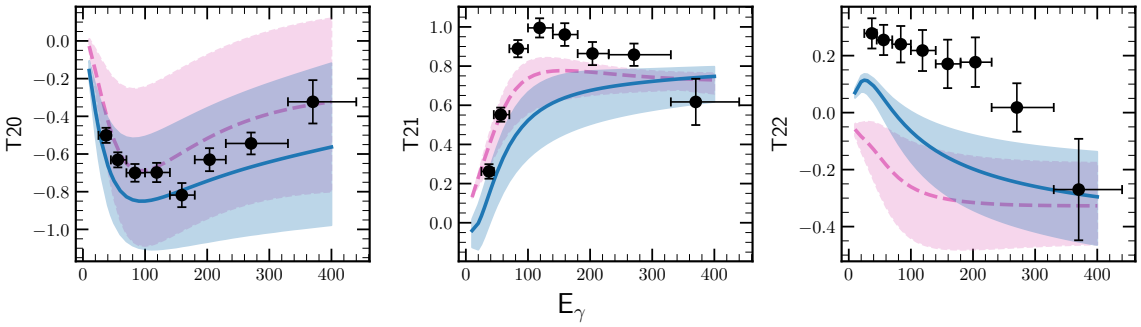

Figure 4.13: Tensor analyzing powers T_{20}, T_{21} and T_{22} as a functions of the photon's energy within the outgoing proton's angle range $24° - 48°$ (in the center of mass frame). Solid blue line is a mean value of my predictions obtained with SMS potential at N^{4}LO+ chiral order and with $\Lambda = 450$ MeV at energy values from 25 to 45 MeV within a given angles range and where SN current was used together with Siegert approach. Pink dashed line is similar prediction but with SN only. The corresponding bands show the deviation of predictions in the regarded energy region. Filled circles are experimental data from [26] for the analogous energy span.

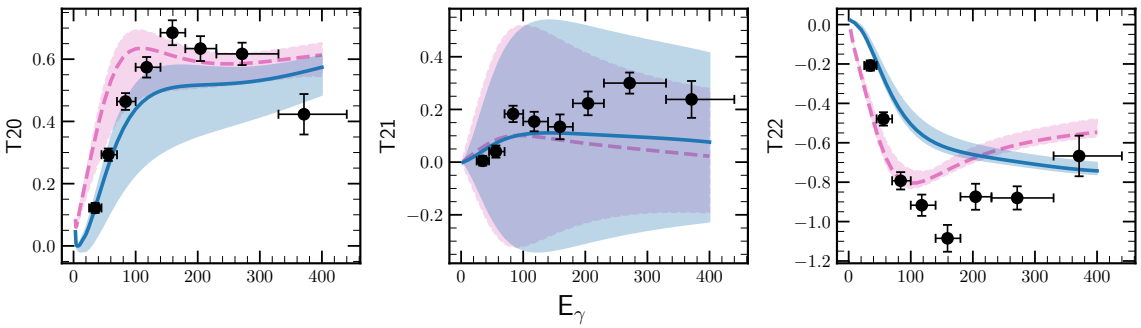

Figure 4.14: The same as on the Fig. 4.13 but for the angles' range $70° - 102°$.

BIBLIOGRAPHY

[1] B.L. Ioffe. Qcd (quantum chromodynamics) at low energies. *Progress in Particle and Nuclear Physics*, 56(1):232–277, 2006.

[2] H Arenhövel and M. Sanzone. Photodisintegration of the deuteron: A Review of theory and experiment. *Few Body Syst. Suppl.*, 3:1–183, 1991.

[3] W. Glöckle. Effects of the two-pion exchange three-nucleon force in the triton and 3he. *Nuclear Physics A*, 381(3):343–364, 1982.

[4] V. G. J. Stoks, R. A. M. Klomp, C. P. F. Terheggen, and J. J. de Swart. Construction of high-quality nn potential models. *Phys. Rev. C*, 49:2950–2962, Jun 1994.

[5] R. B. Wiringa, V. G. J. Stoks, and R. Schiavilla. Accurate nucleon-nucleon potential with charge-independence breaking. *Phys. Rev. C*, 51:38–51, Jan 1995.

[6] A. Nogga, H. Kamada, and W. Glöckle. Modern nuclear force predictions for the α particle. *Phys. Rev. Lett.*, 85:944–947, Jul 2000.

[7] Robert B. Wiringa, V. G. J. Stoks, and R. Schiavilla. An Accurate nucleon-nucleon potential with charge independence breaking. *Phys. Rev.*, C51:38–51, 1995.

[8] V. G. J. Stoks, R. A. M. Klomp, M. C. M. Rentmeester, and J. J. de Swart. Partial-wave analysis of all nucleon-nucleon scattering data below 350 mev. *Phys. Rev. C*, 48:792–815, Aug 1993.

[9] Steven Weinberg. Nuclear forces from chiral lagrangians. *Physics Letters B*, 251(2):288–292, 1990.

[10] Steven Weinberg. Effective chiral lagrangians for nucleon-pion interactions and nuclear forces. *Nuclear Physics B*, 363(1):3–18, 1991.

[11] R. Machleidt and D. R. Entem. Chiral effective field theory and nuclear forces. *Phys. Rept.*, 503:1–75, 2011.

[12] E. Epelbaum, H. Krebs, and U. G. Meißner. Precision nucleon-nucleon potential at fifth order in the chiral expansion. *Phys. Rev. Lett.*, 115(12):122301, 2015.

[13] P. Reinert, H. Krebs, and E. Epelbaum. Semilocal momentum-space regularized chiral two-nucleon potentials up to fifth order. *Eur. Phys. J.*, A54(5):86, 2018.

[14] Carl Gustav Jakob Jacobi. Ueber gauss neue methode, die werthe der integrale näherungsweise zu finden. 1826.

[15] Jun John Sakurai. *Modern quantum mechanics; rev. ed.* Addison-Wesley, Reading, MA, 1994.

[16] Ch. Elster. Physics 755 : Nuclear theory. http://www.phy.ohio.edu/~elster/phys755/index.html. [Online lecture notes].

[17] M. Bosman, A. Bol, J.F. Gilot, P. Leleux, P. Lipnik, and P. Macq. Measurement of the total cross section for the ^{1}H(n, γ) ^{2}H reaction between 37 and 72 mev. *Physics Letters B*, 82(2):212–215, 1979.

[18] Y. Birenbaum, S. Kahane, and R. Moreh. Absolute cross section for the photodisintegration of deuterium. *Phys. Rev. C*, 32:1825–1829, Dec 1985.

[19] R. Moreh, T. J. Kennett, and W. V. Prestwich. ^{2}H(γ,n) absolute cross section at 2754 kev. *Phys. Rev. C*, 39:1247–1250, Apr 1989.

[20] R. Bernabei, A. Incicchitti, M. Mattioli, P. Picozza, D. Prosperi, L. Casano, S. d'Angelo, M. P. De Pascale, C. Schaerf, G. Giordano, G. Matone, S. Frullani, and B. Girolami. Total cross section for deuteron photodisintegration between 15 and 75 mev. *Phys. Rev. Lett.*, 57:1542–1545, Sep 1986.

[21] J. Arends, H.J. Gassen, A. Hegerath, B. Mecking, G. Nöldeke, P. Prenzel, T. Reichelt, A. Voswinkel, and W.W. Sapp. Experimental investigation of deuteron photodisintegration in the δ-resonance region. *Nuclear Physics A*, 412(3):509–522, 1984.

[22] D. M. Skopik, Y. M. Shin, M. C. Phenneger, and J. J. Murphy. Photodisintegration of deuterium determined from the electrodisintegration process. *Phys. Rev. C*, 9:531–536, Feb 1974.

[23] S. Q. Ying, E. M. Henley, and G. A. Miller. DEUTERON PHOTODISINTEGRATION. *Phys. Rev.*, C38:1584–1600, 1988. including references.

[24] E. De Sanctis et al. Deuteron Photodisintegration Cross-section Between 100-MeV and 220-MeV. *Phys. Rev. Lett.*, 54:1639, 1985.

[25] K M Schmitt and H Arenhövel. Deuteron photodisintegration with the bonn OBE potentials. *Few-body syst.*, 7(3):95–117, 1989.

[26] I. A. Rachek, L. M. Barkov, S. L. Belostotsky, V. F. Dmitriev, M. V. Dyug, R. Gilman, R. J. Holt, B. A. Lazarenko, S. I. Mishnev, V. V. Nelyubin, D. M. Nikolenko, A. V. Osipov, D. H. Potterveld, R. Sh. Sadykov, Yu. V. Shestakov, V. N. Stibunov, D. K. Toporkov, H. de Vries, and S. A. Zevakov. Measurement of tensor analyzing powers in deuteron photodisintegration. *Phys. Rev. Lett.*, 98:182303, May 2007.

[27] S.I. Mishnev, D.M. Nikolenko, S.G. Popov, I.A. Rachek, A.B. Temnykh, D.K. Toporkov, E.P. Tsentalovich, B.B. Wojtsekhowski, S.L. Belostotsky, V.V. Nelyubin, V.V. Sulimov, and V.N. Stibunov. Measurement of the analyzing power components in photodisintegration of the polarized deuteron. *Physics Letters B*, 302(1):23–28, 1993.